Journal of Sound and Vibration 332 (2013) 3377–3389

Contents lists available at SciVerse ScienceDirect

Journal of Sound and Vibration

journal homepage: www.elsevier.com/locate/jsvi

Theoretical and experimental analyses of a nonlinear magnetic vibration isolator with quasi-zero-stiffness characteristic

Daolin Xu [a,*], Qiping Yu [b], Jiaxi Zhou [a], S.R. Bishop [c]

[a] State Key Lab of Advanced Design and Manufacturing for Vehicle Body, College of Mechanical and Vehicle Engineering, Hunan University, Changsha, China
[b] Beijing Automotive Technology Center, Beijing, China
[c] Department of Mathematics, University College London, Gower Street, London WC1E 6BT, UK

ARTICLE INFO

Article history:
Received 1 November 2012
Received in revised form
22 January 2013
Accepted 26 January 2013
Handling Editor: L.G. Tham
Available online 26 March 2013

ABSTRACT

This paper presents a nonlinear magnetic low-frequency vibration isolator designed with the characteristic of quasi-zero stiffness (QZS). An approximate expression of the magnet repulsive force is proposed and a unique analytical relationship between the stiffness of vertical spring and initial gap settings of the magnet springs is derived for the QZS system. Based on the harmonic balance (HB) method, the force transmissibility is formulated and the jumping frequencies, effect of excitation force and damping ratio are discussed for characteristic analysis. An experimental prototype is developed and tested. The performance of the QZS system is verified through a series of experimental studies showing that the new model greatly outperforms standard linear isolation systems especially in low-frequency domain. The tuning techniques for adapting to the change of loading mass and adjusting the QZS property in practice are also addressed.

1. Introduction

In many practical examples in engineering, vibrations are more than often thought to induce harmful effects reducing the performance of machines and are thus undesirable [1]. One of the most common approaches of attenuating unwanted vibrations is to use passive isolation devices [2]. In the ideal case of a mass m supported by an elastic element with stiffness, k, on a rigid foundation, a linear isolator can only provide efficient attenuation when an excitation frequency is greater than $\sqrt{2k/m}$ [1,2]. It is evident that a smaller stiffness leads to a broader frequency band of vibration isolation but usually encounters the problem of a larger static displacement of the supported mass [3,4]. In recent years quasi-zero stiffness (QZS) systems have been developed to overcome this disadvantage. A quasi-zero stiffness system possesses a localized zero stiffness at the equilibrium state. As the deflection increases, the stiffness increases nonlinearly with the characteristics of a high-static-low-dynamic stiffness system. QZS systems offer the desirable property to satisfy the requirement of a low natural frequency but small static displacement [5].

There are a number of ways to achieve a QZS property by making use of positive and negative stiffness. Ibrahim [6] reviewed the recent advances in nonlinear passive vibration isolators in detail. A typical form of a QZS isolator was designed by connecting a vertical coil spring and two oblique coil springs [1,2,5]. Many other methods of constructing a QZS system include using six rods and a tension spring [7], combining positive and negative stiffness with a compressed

* Corresponding author. Tel.: +86 15111293108.
E-mail address: dlxu@hnu.edu.cn (D. Xu).

0022-460X/$ - see front matter © 2013 Elsevier Ltd. All rights reserved.
http://dx.doi.org/10.1016/j.jsv.2013.01.034

rod [8], designing a nonlinear ultra-low frequency horizontal vibration isolation system (VIS) with parallel positive and inverse pendulums [9], combining a beam subject to an axial load with a positive stiffness spring [10]. In Refs. [11,12], they showed that a highly deformed pinched loop possesses a softening stiffness. In [13], structural buckling of axially loaded rods was utilized to improve vibration isolation of a vehicle driver seat. Magnetic springs were introduced to QZS systems incorporating different prototypes, including the model of using two linear coil springs and three permanent magnets arranged in an attracting configuration [14], two pairs of magnets [15] and a floating magnet interacting with two fixed permanent magnets [16]. In [17], the QZS property of the isolator was obtained by connecting a mechanical spring, in parallel with a magnetic spring that is constructed by a pair of electromagnets and a permanent magnet.

This paper investigates a QZS system based on a prototype of combining an appropriate vertical coil spring (positive stiffness) with two pitched bars connected with magnet springs (negative stiffness). The motivation for building these magnetic springs is that the magnets enable the nonlinear repulsive forces to be adjusted flexibly by tuning the distance between the two opposite magnets, which can then easily reach the condition of the quasi-zero stiffness feature, as explained in the following section. In addition, the non-contact nature of the forces induced by the magnets offers easy assembly within the system. The configuration and structural arrangement of permanent magnetic springs exhibit strongly nonlinearity. Pre-stressed, vertical springs can satisfy the requirement of a variable isolation mass under different operating conditions.

The aim of this paper is to develop an analytical model with a matching physical model for experimental verification for the passive QZS isolator that could be useful for applications of a time delay control using electromagnets instead of permanent magnets in future study. The rest of the paper is organized as follows: in Section 2, the proposed permanent magnet spring is introduced. Section 3 gives the characterization of the QZS vibration isolation system. In Section 4, the simulation results of the system are presented, including dynamic analysis and force transmissibility. The experimental setup and the experimental results are shown in Section 5. Finally, in Section 6, some conclusions on the performance of the designed isolation system are addressed.

2. The characteristics of the magnet spring components

The magnetic spring is a key component in the design of a QZS vibration isolation system. We consider a magnetic spring by using a magnetic repulsive force when coupling two magnets by placing the same poles facing each other. Here we utilize the expression of the repulsive force between two permanent magnets given by

$$F = \frac{B_g^2 A_g}{2\mu_0} \tag{1}$$

according to Ref. [18], where F is the repulsive force between the two permanent magnets (N), B_g the flux density in the air gap between the two permanent magnets (Wb/m^2), A_g the area of the face of the magnet which is acted on by the repulsive force (m^2) and μ_0 the absolute magnetic permeability in a vacuum ($4\pi \times 10^{-7}$ H/m).

The flux density B_g in the air gap is given by

$$B_g = B_r\left(1 - \frac{L_g}{\sqrt{L_g^2 + D^2}}\right) \tag{2}$$

where B_r is the residual flux density (Tesla or G) and L_g the air gap between two permanent magnets (m or cm).

Note that the above expressions are based on the theoretical assumptions on an ideal magnetic circuit. To calculate the exact force for any particular two magnets is not straightforward requiring knowledge of the leakage flux, the reluctance (or magnetic resistance) and the operating point of the dispersion and so on. Other analytical forms in the description of magnetic force are available [19–21] but too complex to use for the later theoretical analysis of the QZS system dynamics, all of which means that precise determination of this force is often impractical. Consequently, in what follows, we shall introduce an empirical method to characterize the force between two magnets.

Two equal sized magnets with the same physical properties are considered. One is fixed while the other is placed directly above with the same polarity facing the fixed magnet. The two magnets are aligned and centralized with a common smooth guide-rod through the magnet center holes. The magnetic repulsive force holds the upper magnet in a floating state, as shown in Fig. 1.

To measure the repulsive force pertaining to the distance between two magnets, an experiment was carried out by gradually adding a static load to the floating magnet. The disk-shaped magnet is made of NdFeB material with the grade N35, and the outer diameter is of 60 mm, the diameter of the center hole is 10 mm and the thickness 10 mm. For each increase in load, the displacement of the floating magnet is recorded. The relation between the repulsive force and the distance is shown in Fig. 2. According to Ref. [22], the repulsive force between two permanent magnets of equal size can be assumed to be inversely proportional to the nth power of the distance of the two permanent magnets. However, this formula does not appear to be suitable for the particular magnet used in this specific experiment. After having tried

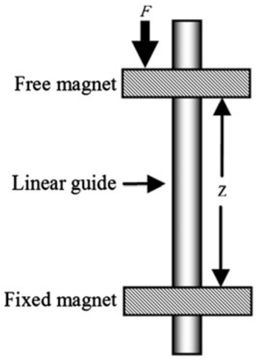

Fig. 1. Schematic representation of the permanent magnet spring.

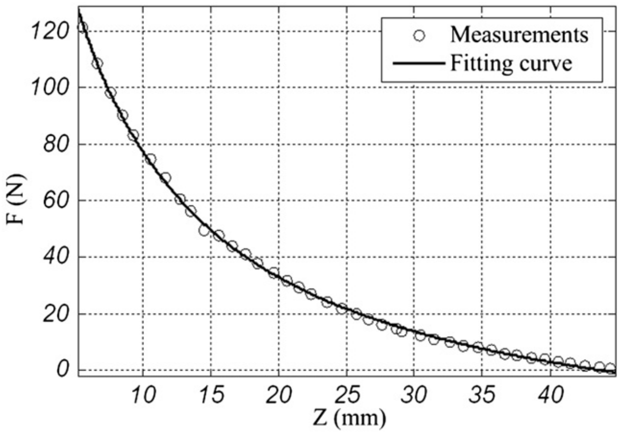

Fig. 2. Repulsive force between the two magnets; measured values (open circles); and the best-fit curve (solid line).

different equations to fit the data, in a least squares sense, an equation of the form given by

$$F = (p_1 \times Z + p_2)/(Z + p_3) \tag{3}$$

was found to be the simplest that provides an excellent match with the data, as seen in Fig. 2, where F is the repulsive force between two permanent magnets (N), p_1 the magnetic coefficient 1 (N), Z the center distance between the two permanent magnets (mm), p_2 the magnetic coefficient 2 (N mm) and p_3 the magnetic coefficient 3 (mm).

Using the experimental data recorded, then the least square method in form of Eq. (3) gives the following coefficients:

$$p_1 = -35.43 \text{ N} \quad p_2 = 1551 \text{ N mm} \quad p_3 = 5.505 \text{ mm} \tag{4}$$

so that the repulsive force between two permanent magnets is formulated as

$$F = (-35.43 \times Z + 1551)/(Z + 5.505). \tag{5}$$

note that this expression may only be suitable for the particular magnets used in this experiment. There are other fitting expressions for magnetic force, and interested readers can refer to the Ref. [23].

3. The QZS vibration isolation system

A QZS property is generally achievable using the mechanism of combining a negative stiffness element with a positive stiffness element. A number of configurations have already been reviewed in the introduction. Here we use a specific QZS system designed by combining two permanent magnet springs aligned in the horizontal direction with one linear vertical coil spring as shown in Fig. 3a in its unloaded condition. Two connecting rods are joined at the point A with a vertical stressed linear coil spring of stiffness k. In addition, the coil spring is pre-stressed, i.e. compressed by length δ. The other end of the connecting rod is connected to the free magnet through a hinged joint. The coordinate x defines the displacement of point A from the initial unloaded position. When a mass is loaded at the point A, the vertical coil spring is compressed downwards and the two oblique connecting rods push the two free magnets sliding apart along the linear guide. Under a suitably sized load, point A may reach the position at $x = h$ (point B), which is referred to as an equilibrium position while the connecting rod is forced to be in the horizontal position. In this regard, the static load is only supported

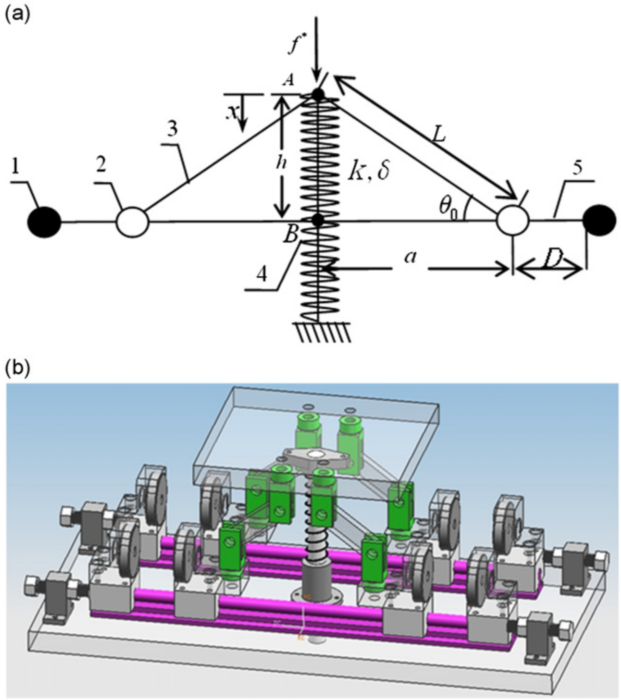

Fig. 3. (a) Schematic representation of the QZS system in the initial position before loading a mass. 1-Fixed magnet, 2-free sliding magnet, 3-connecting rod, 4-coil spring, and 5-linear guide. (b) Prototype model of the proposed isolation system.

by the vertical spring k at the static equilibrium position. When the system is designed in this way, the two permanent magnet springs together provide a negative stiffness in the vertical direction and counteract the positive stiffness of the vertical coil spring. In this way, a QZS system is developed. The motion about this equilibrium position is the primary interest of this paper.

3.1. Force–displacement characteristic of the two coupled magnet springs

Consider the QZS vibration isolation system in Fig. 3a, in the absence of the vertical coil spring k. The rods connecting the free magnets and the point A have initial length L and can rotate around the hinged joint. The symbol a and symbol h represent the horizontal and the vertical distance from the centers of free magnets to point A, respectively. The initial distance between two magnets is D. The connecting rods are initially set at an angle θ_0 from the horizontal. A static force f^* is applied at the point A. In the vertical direction, the forces on the connecting rods, via two permanent magnet springs, balance the applied force. This implies that

$$f^* = 2F \tan\theta \tag{6}$$

where F is the force of the permanent magnet spring, and $\tan\theta = (h-x)/\sqrt{L^2-(h-x)^2}$. When the free magnet moves along the linear guide with the distance Z from the fixed magnet, noting that $L^2 = h^2+a^2$, $Z = a+D-\sqrt{L^2-(h-x)^2}$ and $F = (p_1 \times Z+p_2)/(Z+p_3)$, Eq. (6) can be written as

$$f^* = 2 \times \frac{p_1 \times (a+D-\sqrt{L^2-(h-x)^2})+p_2}{a+D-\sqrt{L^2-(h-x)^2}+p_3} \times \frac{h-x}{\sqrt{L^2-(h-x)^2}} \tag{7}$$

note that the force f^* will tend to be zero as $x \to h$ when the free magnets slide to the extreme ends.

3.2. A QZS vibration isolation system

Including the linear vertical coil spring k in the system, as shown in Fig. 3a, the force f of the QZS system can be given by

$$f = f^* + kx + k\delta \tag{8}$$

the displacement is set as $y=x-h$ from the equilibrium, and Eq. (8) becomes

$$f=ky+kh+k\delta-2\times\frac{p_1\times(a+D-\sqrt{L^2-y^2})+p_2}{a+D-\sqrt{L^2-y^2}+p_3}\times\frac{y}{\sqrt{L^2-y^2}} \tag{9}$$

the stiffness of the system can be found by differentiating Eq. (9) with respect to the displacement y, and gives

$$K=k-\frac{2y^2(p_1p_3-p_2)}{(L^2-y^2)(a+D+p_3-\sqrt{L^2-y^2})^2}-\frac{2L^2(p_2+p_1(a+D-\sqrt{L^2-y^2}))}{(L^2-y^2)^{3/2}(a+D+p_3-\sqrt{L^2-y^2})} \tag{10}$$

there is a unique relationship between the initial inter-magnetic distance, D, and the vertical coil spring k that yields the desired stable QZS characteristic. If Eq. (10) is evaluated at the static equilibrium position $y=0$ then setting $K=0$ yields the stiffness value k_{qzs} of the coil spring that gives quasi-zero-stiffness is

$$k_{qzs}=\frac{2p_2+2p_1(a+D_{qzs}-L)}{L(a+D_{qzs}-L+p_3)} \tag{11}$$

the initial inter-magnetic distance D, marked as D_{qzs} when the property of quasi-zero-stiffness holds, can be expressed as

$$D_{qzs}=L+\frac{2p_2-k_{qzs}Lp_3}{k_{qzs}L-2p_1}-a \tag{12}$$

the stiffness of the QZS system can be written as

$$K_{qzs}=k_{qzs}-\frac{2y^2(p_1p_3-p_2)}{(L^2-y^2)(a+D_{qzs}+p_3-\sqrt{L^2-y^2})^2}-\frac{2L^2(p_2+p_1(a+D_{qzs}-\sqrt{L^2-y^2}))}{(L^2-y^2)^{3/2}(a+D_{qzs}+p_3-\sqrt{L^2-y^2})} \tag{13}$$

the stiffness K_{qzs} varies as a function of the displacement y, plotted in Fig. 4 for several values of the initial inter-magnetic distance D. Here, the values of parameters of the system are as shown in Table 1.

For $D<D_{qzs}$, the connecting rods dominate the behavior resulting in a region of negative stiffness. For $D>D_{qzs}$, the stiffness of the system is always positive and exhibits weak nonlinearity. A unique intermediate value of $D=D_{qzs}$ exists which corresponds to a stable equilibrium position with zero stiffness. This condition occurs at the equilibrium position $y=0$ where the negative stiffness from the two oblique connecting rods is exactly counteracted by the positive stiffness of the vertical coil spring. This can be seen more clearly in Fig. 4, in which the stiffness of whole system is plotted as a function of displacement for the same set of parameter values.

From Eqs. (11) and (12), it can be seen that the QZS characteristic of the proposed system can be adjusted by regulating the initial inter-magnetic distance D when the initial geometry parameters (a and L) and vertical spring k_{qzs} are kept the constant. Fig. 5 illustrates how the value of stiffness k_{qzs} of the linear vertical coil spring is dependent on the initial inter-magnetic distance D_{qzs}. As the value of k_{qzs} decreases, the appropriate distance D_{qzs}, which leads to QZS characteristic, also reduces.

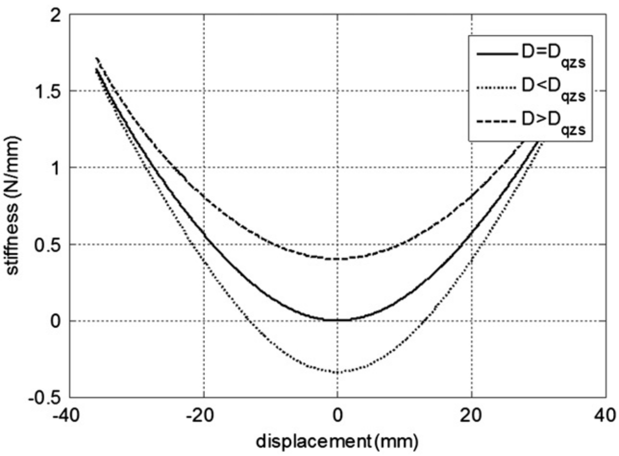

Fig. 4. Stiffness of the system when $D<D_{qzs}$, $D=D_{qzs}$ and $D>D_{qzs}$.

Table 1
The physical parameters of the proposed system.

Parameter	Value
m	5.8745 kg
δ	24 mm
a	48 mm
L	60 mm
k_{qzs}	0.9595 N/mm
D	33.7 mm

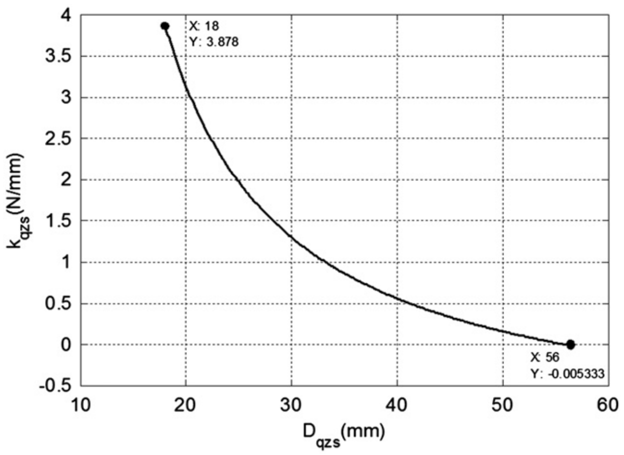

Fig. 5. Relationship between initial magnetic distance D_{qzs} and the linear vertical coil spring k_{qzs}.

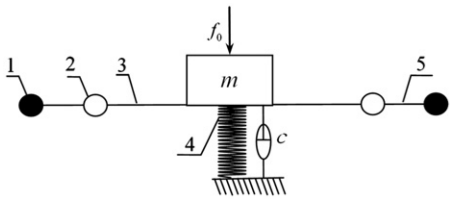

Fig. 6. Schematic representation of the QZS system in the actual operating position (equilibrium state) after loading a mass; 1-fixed magnet, 2-free magnet, 3-connecting rod, 4-coil spring, and 5-linear guide.

3.3. QZS vibration isolation system with a suitably sized mass supported

The QZS system shown in Fig. 6 is loaded with a suitably sized mass such that at the static equilibrium position ($y=0$) the inclined connecting rods are in the horizontal position. Initially, at the static equilibrium position, the mass is held in equilibrium by the compression force of the vertical spring. The gravity force acting on the mass is counter balanced by the compression force of vertical spring. Therefore, the support load capacity in this system depends only on the stiffness of the vertical spring k_{qzs} and its initial deformation $(h+\delta)$. When the stiffness of the system is designed to be zero at the static equilibrium position, then the quantity of the mass can be determined by

$$m = k_{qzs}(h+\delta)/g \tag{14}$$

if a particular mass is to be isolated, we can employ Eq. (14) to determine suitable parameters for the design of a QZS vibration system. In applications, the value of the isolation mass may be changed under different operating conditions. In this case, the inclined connecting rods may not be in the horizontal position at the static equilibrium position. Therefore the isolation system will not have the zero stiffness characteristic at the static equilibrium position. Thus, the effectiveness of the vibration isolation of the proposed system will be reduced. However, Eq. (14) shows the parametric dependence between the isolation mass m and the pre-stressed length δ of vertical spring. If this isolation system is prototyped, the geometry parameter h and the stiffness of vertical spring k_{qzs} cannot be changed easily, but the pre-stressed length δ can be adjusted simply to make the connecting rods in horizontal position. Then the proposed system can maintain the QZS characteristic at static equilibrium position.

3.4. Approximation to the stiffness of the QZS vibration isolation system

It would considerably simplify the subsequent dynamic analysis of the QZS system if its stiffness could be described in a polynomial form. A simplified cubic expression of the force is therefore sought.

Eq. (9) can be expanded using the Taylor Series up to the third order

$$f = f(0) + f'(0)y + \frac{f''(0)y^2}{2!} + \frac{f'''(0)y^3}{3!} + \cdots \tag{15}$$

where $y=0$ is the point about which the function is expanded. Since the displacement of the system about the static equilibrium position is of interest, the power series for the force is expanded about this point

$$f = f(0) + K_{qzs}(0)y + \tfrac{1}{2}K'_{qzs}(0)y^2 + \tfrac{1}{6}K''_{qzs}(0)y^3 \tag{16}$$

where

$$f'(0) = K_{qzs}(0),\ f''(0) = K'_{qzs}(0) \text{ and } f'''(0) = K''_{qzs}(0).$$

if a and L are chosen according to Eq. (11), then Eq. (13) can be written as

$$K_{qzs}(0) = 0 \tag{17}$$

differentiating Eq. (13) with respect to y gives $K'_{qzs}(y)$ and when $y=0$, it leads to

$$K'_{qzs}(0) = 0 \tag{18}$$

further differentiating $K'_{qzs}(y)$ with respect to y to obtain $K''_{qzs}(y)$, at $y=0$, it reduces to

$$K''_{qzs}(0) = -\frac{6p_1}{L^2(a+D+p_3-L)} + \frac{6(p_2+p_1(a+D-L))}{L^2(a+D+p_3-L)^2} - \frac{6(p_2+p_1(a+D-L))}{L^3(a+D+p_3-L)} \tag{19}$$

moreover, if the force is transformed by $f_1 = f - f(0)$, substituting Eqs. (17)–(19), then Eq. (16) becomes

$$\begin{aligned} f_1 &= \tfrac{1}{6}K''_{qzs}(0)y^3 \\ &= \frac{1}{6}\left(-\frac{6p_1}{L^2(a+D+p_3-L)} + \frac{6(p_2+p_1(a+D-L))}{L^2(a+D+p_3-L)^2} - \frac{6(p_2+p_1(a+D-L))}{L^3(a+D+p_3-L)}\right)y^3 \end{aligned} \tag{20}$$

the approximate stiffness of the QZS system is given as

$$\begin{aligned} K_{QZS\_app} &= \frac{df_1}{dy} = \tfrac{1}{2}K''_{qzs}(0)y^2 \\ &= \frac{1}{2}\left(-\frac{6p_1}{L^2(a+D+p_3-L)} + \frac{6(p_2+p_1(a+D-L))}{L^2(a+D+p_3-L)^2} - \frac{6(p_2+p_1(a+D-L))}{L^3(a+D+p_3-L)}\right)y^2 \end{aligned} \tag{21}$$

Eq. (21) contains a square term of the displacement y. Fig. 7 shows the approximate solution (dot line) along with the analytical solution (solid line) as well as Carrella's three coil spring model [1] (dashed line), where the parameters of the system are taken as the same as before.

The global trends of the three curves are generally agreeable to each other. In fact, the actual vibration amplitude of the underlying system in experiments is in the scale of millimeters. Considering a vibration oscillation range within 2 mm, the

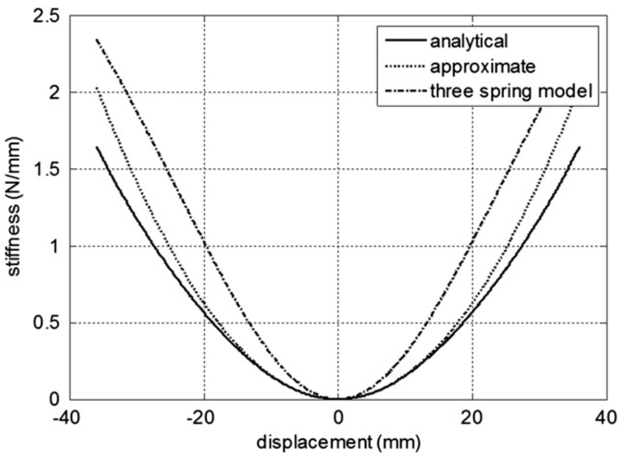

Fig. 7. Solutions of the QZS system stiffness; analytical solution (solid line); and approximate solution (dotted line). A three-spring model of a QZS mechanism [1] (dashed–dotted line).

maximum difference between the analytical and approximated curves is remained within 2 percent error around the static equilibrium position $y=0$. This approximation is valuable when it involves subsequent dynamic analysis.

4. Numerical simulations and analysis

The dynamic performance of the QZS vibration isolation system, including the response of amplitude–frequency equation and force transmissibility of vibration isolation, may be studied by employing the harmonic balance (HB) method. The operation process is based on the condition that the vertical spring and the two magnet springs are always in compression. When the mass performs an oscillation driven by an excitation force, then the force is transmitted from the isolating equipment to the base through the vertical spring and the damper. The transmitted force to the base depends on the dynamic stiffness of the isolation system.

In this paper, the values of parameters of the proposed system are taken as in Table 1. Fig. 7 plots the stiffness curves of the QZS system which includes Carrella's model [1]. The reason for including Carrella's model here is for a comparison of the stiffness characteristics between the proposed magnet springs and linear coil springs in [1] because the geometry structure of two QZS systems is similar. As clearly seen from Fig. 7, the global trend is similar but in the extreme case of oscillation level of 36 mm, there is about 20 percent difference in stiffness between the approximated magnetic model and Carrella's model. However, considering actual vibration in millimeters scale, the difference in stiffness between the two systems is obviously much less than 5 percent within a vibration amplitude of 2 mm, when the initial geometry parameters (a and h) and the linear vertical coil spring k_{qzs} are held the same as in [1]. It means that the stiffness of our model based on magnetic springs is relatively softened about 5 percent. Note that the stiffness depends on the parameters chosen in prototype design, and it is not necessary implying that the magnetic QZS system can generally offer a more soften characteristic than that of coil spring ones. The proposed system delivers an improved softening characteristic about the static equilibrium than the three-spring model, which may benefit the low frequency isolation.

4.1. Dynamic response of the QZS system

The system consists of a mass, a linear damper with damping coefficient c, a coil spring and two magnetic springs. When an exciting force f_0 is applied to the mass, the mass oscillates around the equilibrium position. The following hypotheses are applied that the displacement about the static equilibrium position is small; the restoring force can be expanded using the Maclaurin series up to third order; the system is optimized such that the system has zero stiffness at the static equilibrium position. The equation of motion of the system about the static equilibrium position can be approximated by Duffing's type of equation without a linear term. For harmonic excitation, the non-dimensional equation of motion is given by

$$\ddot{\hat{y}}+2\zeta\dot{\hat{y}}+\gamma\hat{y}^3=\hat{f}\cos(\Omega\tau) \tag{22}$$

where

$$\hat{k}=\frac{1}{6}K''_{qzs}(0),\ \hat{y}=\frac{y}{L},\ \omega_0^2=\frac{k_{qzs}}{m},\ \tau=\omega_0 t,\ \zeta=\frac{c}{2m\omega_0},\ \Omega=\frac{\omega}{\omega_0},\ \gamma=\frac{\hat{k}L^2}{m\omega_0^2},\ \hat{f}=\frac{f_0}{k_{qzs}L}$$

to investigate the dynamic behavior of the QZS system the HB method is used to determine its approximate analytical response at the excitation frequency. The reasons for this choice are its simplicity and applicability to strongly nonlinear systems [24–26]. In this study, the attention is restricted to the system parameters for which the frequency of response is predominantly the same as that of the harmonic excitation, so that all other insignificant frequency components are neglected. The solution of Eq. (22) is assumed to be $\hat{y}=A\cos(\Omega\tau+\varphi)$, and it yields the characteristic equation

$$(-\Omega^2A+\tfrac{3}{4}\gamma A^3)^2+(-2\zeta\Omega A)^2=\hat{f}^2 \tag{23}$$

the force amplitude of the excitation frequency is $\hat{f}$. The force transmitted through the QZS appliance and the damper is given by

$$f_t=\gamma\hat{y}^3+2\zeta\dot{\hat{y}}=\gamma A^3\cos^3(\Omega\tau+\varphi)-2\zeta\Omega A\sin(\Omega\tau+\varphi) \tag{24}$$

the magnitude of the transmitted force is given by

$$F_t=\sqrt{(\tfrac{3}{4}\gamma A^3)^2+(2\zeta\Omega A)^2} \tag{25}$$

of interest in this section is the amplitude of the force transmissibility, which is defined as the ratio of the magnitude of the force transmitted to the rigid foundation, to the magnitude of the excitation force. The force transmissibility is given by

$$T=\frac{F_t}{\hat{f}}=\frac{\sqrt{(\tfrac{3}{4}\gamma A^3)^2+(2\zeta\Omega A)^2}}{\hat{f}} \tag{26}$$

4.2. Comparison between the QZS system and linear system

In order to compare the performance between the designed QZS system and the corresponding linear system, we consider isolating the same mass under the same external excitation conditions. The linear system is obtained from the proposed system by removing the two permanent magnet springs. Thus we keep the isolation mass constant, and design the system parameters according to Eq. (11) for the QZS system. Eq. (26) implies that the smaller value of parameter γ leads to lower force transmissibility of the QZS system. The QZS system performs vibration isolation after the jump-down frequency according to Ref. [5]. The value of the frequency depends on excitation force, damping ratio and stiffness. In order for the QZS system to outperform the linear system, the jump-down frequency must hold to be smaller than the natural frequency of the linear system. Thus we have the condition defined by the inequality (27).

$$\hat{f} < \frac{4\zeta}{\sqrt{3\gamma}} \tag{27}$$

to understand the performance of vibration isolation between the nonlinear QZS system and linear system, Fig. 8 shows the characteristics via the transmissibility against Ω. The physical parameters are used in the numerical calculation listed in Table 2. The harmonic excitation is sinusoidal and the excitation frequency ranges from 0.1 Hz to 10 Hz.

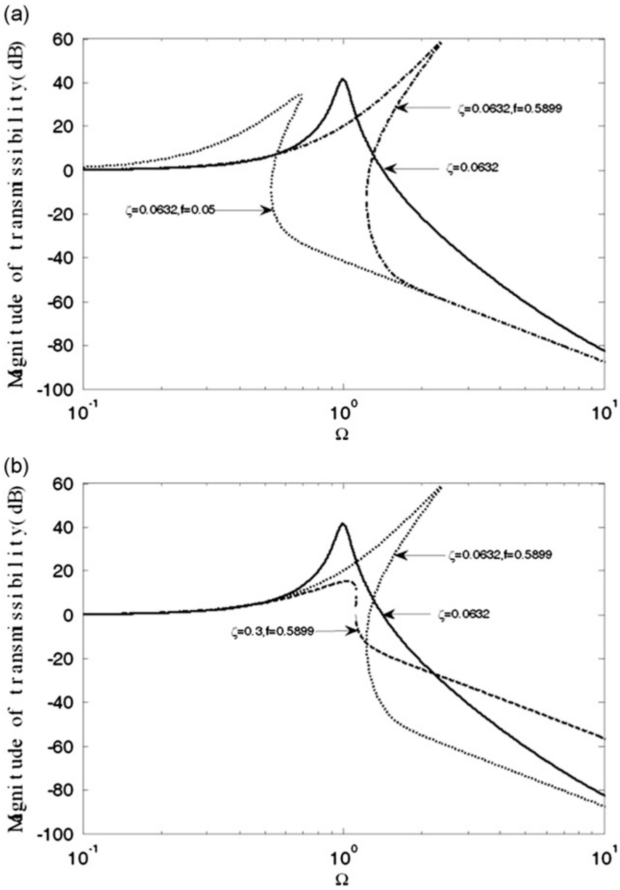

Fig. 8. Transmissibility of QZS system and linear system versus the non-dimensional excitation frequency for different values of (a) excitation force $\hat{f}$ and (b) damping ζ.

Table 2
The physical parameter of the system used for simulation.

Parameter	Value
γ	1.9613
ζ	0.0632, 0.3
$\hat{f}$	0.05, 0.5899

The transmissibility of QZS system is computed by Eq. (26). The solid line shows the response of the linear system and other lines denote for the QZS system.

Consider the case of the parameter $\zeta = 0.0632$ and changing the excitation force $\hat{f}$ from 0.05 to 0.5899. When the non-dimensional excitation force increases, the transmissibility of QZS system also increases. The least frequency for which a vibration can be isolated is increased from 0.69 Hz to 2.37 Hz. The greater jump-down frequency means that the region for isolating vibration is reduced as shown in Fig. 8a. The damping effect is also indicated in Fig. 8b. When setting the parameter $\hat{f} = 0.5899$, and increasing the damping ζ from 0.0632 to 0.3, the result is that the jump-down frequency and the peak value of the transmissibility curve are decreased. In this case, however, the transmissibility increases when excitation involves in higher frequency domain, meaning the vibration attenuation becomes worse in the high frequency region. It is common that damping always degrades the efficiency of vibration attenuation in high frequency domain.

We do not include Carrella's model for comparison here because the difference of the stiffness characteristic between our model and Carrella's model shown in Fig. 7 is insignificant within 5 percent based on numerical computation under millimeter scale vibration. Thus we can expect theoretically that the two models are almost *equivalent* in vibration isolation performance based on transmissibility in Eq. (26). Since our model is slightly more softening than Carrella's model by about 5 percent, our model should slightly improve the performance of force transmissibility but less than 5 percent for sure. The improvement varies within this range also dependent on other conditions of vibration amplitude, damping and frequency.

5. Experiment apparatus and results

5.1. Experimental setup

In this section, a prototype experiment is investigated that was specifically built for this study to verify the isolation performance of the proposed system and the physical parameters are listed in Table 1. Fig. 9 shows the experimental setup for the proposed QZS system. The mass is supported by the vertical spring and moves in the vertical direction through the guide rod and bushing. Two magnet springs, each of which comprises two permanent magnets and slide blocks in series as shown in Fig. 9a, are symmetrically arranged on the linear guide. At the static equilibrium position, the connecting rods are placed in a horizontal position. The initial distance between the two magnets of the magnet spring can be tuned by the gap tuning device at the two ends of the linear guide. An appropriate initial magnet distance can be adjusted to ensure the system having the QZS characteristic. The gap tuning device comprises a screw and a pedestal. The pedestal is fixed on the base. The fixed magnet is positioned by the adjustable screw.

An exciter is placed on the top of the rig to provide external excitation. In between the exciter and the mass a force sensor is installed to measure the excitation force in experiments. Another force sensor is placed underneath the base to measure the transmitted force. Thus we are able to estimate the transmissibility during experiments.

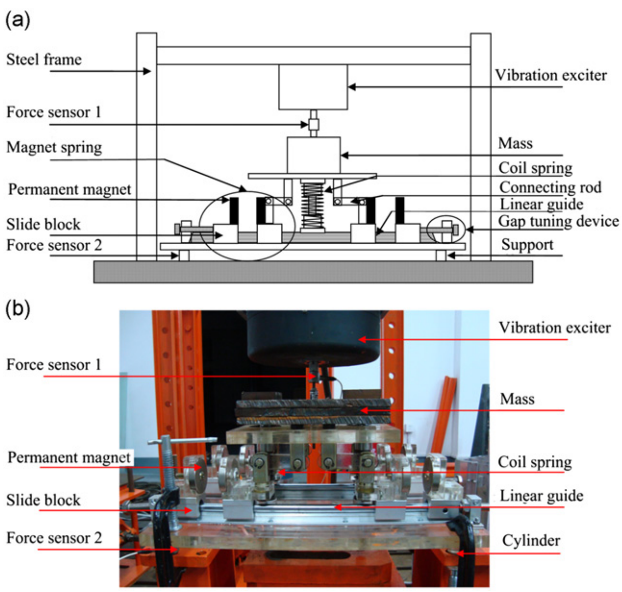

Fig. 9. Experimental setup. (a) Schematic representation of the experimental system; (b) prototype of the experimental apparatus.

5.2. Experiment results

This section presents the isolation performance observed from the experiments to compare the linear system and the proposed QZS system. The mass is excited in the vertical direction. At the same time the force between the isolation system and the rigid base was recorded by a force sensor. The isolation system is supported by a sensor and three cylinders which are made of plexiglass. The plexiglass cylinder is the same size as the force sensor. Four support points are symmetrically placed at the four corners of the QZS system as Fig. 9b shows. As the layout of the whole QZS system is axisymmetric, the root mean square (RMS) value of the force transmitted from every support is regarded as being the same. Therefore, the total transmitted force from the whole QZS system to the rigid foundation is four times of the force measured by force sensor.

The force transmissibility in the frequency domain, which is defined to be the ratio of the RMS [27] of transmitted force $|F_t|$ to excitation $|\hat{f}|$, is recorded. In this case when the excitation signal is sinusoid, the recorded RMS force amplitude and excitation frequency are given in Table 3. In the experiments, the system can also be excited with a constant force to allow comparison. When a periodic force is applied and the excitation frequency region is varied from frequency 4.5 Hz to 20 Hz, the exciter can provide a constant exciting force of RMS 33.961 N. However, in the low frequency region from 0.5 Hz to 4 Hz in the experiments, it is difficult to obtain a constant output of excitation force even if the exciter works with a large oscillating displacement. Therefore, only using smaller RMS amplitudes of excitation force is necessary.

The experimental results for the transmissibility of force were recorded as shown in Fig. 10. The solid curve describes the transmissibility of the corresponding linear system against excitation frequency and the other provides the transmissibility of the QZS system. It reveals that the transmissibility due to using the QZS system has been much improved around the linear resonance frequency. It is because the fact that the stiffness of the QZS system about the equilibrium state is close to zero so that the resonance peak has shifted to lower frequencies and is much smaller than the linear resonance frequency at about 2.4 Hz. The QZS system can attenuate the vibration starting from 1.5 Hz where the transmissibility value is less than one, while the linear system only enables vibration attenuation starting from about 3.5 Hz. This indicates the excellent performance of the QZS system. The QZS system can extend the vibration isolation to a much lower frequency, which has always been seen as a difficult problem for conventional technology. It is interesting to note that in the transmissibility curves the attenuation ability of the QZS system is almost equivalent to, or even slightly less successful than that of the linear system after 7 Hz. In fact, if the damping of the two systems is the same, then in numerical simulations at least, the tendency of attenuation ability is also the same in high frequency domain, see Fig. 8. The reason for the slight difference could be that the actual damping of the QZS system is larger than the linear one because the QZS system has additional mechanical parts, especially the joints connecting the rods which provide friction damping to the system. In experiments, it was observed that the damping effect on the performance of the QZS system is sensitive. Reduction of damping is an important issue for the performance of the QZS system. Low levels of damping can improve the quality of attenuation when high frequencies are involved and can increase effective isolation domain in the low frequency band. In Fig. 10, there is a small peak around 17 Hz for the QZS system. The moving parts, including the sliding blocks and connecting rods, mean that the system is no longer a single degree of freedom system.

Table 3
The RMS amplitude of excitation for different frequency in experiment.

Frequency (Hz)	0.5	1	1.5	2	3	3.5	4	4.5–20
Excitation (N)	2.565	5.497	7.021	9.471	20.055	27.138	30.924	33.961

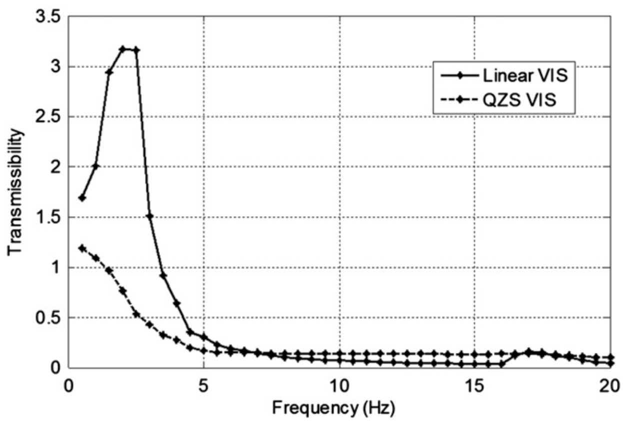

Fig. 10. Experimental results of force transmissibility of the QZS system and the linear system.

Finally we would like to briefly address the tuning procedure adapting to the possible change of mass loaded onto the system. When the geometric configuration is determined, the ratio of the stiffness between the coil spring and magnetic springs has to be fixed to satisfy the requirement the QZS property. There are two approaches to tune the system subjected to the change of loading mass. As loading mass increases for example, the first approach is that we can pre-stress the coil spring by lifting the support base of the coil spring upwards a certain distance until the loading mass is positioned at the equilibrium state. In this procedure, the stiffness of the coil spring and magnetic springs are remained the same. Practically, we can tune the support base through a mechanical mechanism until the rods connected to magnetic springs are positioned horizontally. The second approach is to change the stiffness of the coil spring and magnetic springs simultaneously. When the stiffness of the coil spring increases to adapt to the increase of loading mass, the magnetic springs should be adjusted accordingly to satisfy the requirement of a constant ratio of stiffness. The stiffness of the magnetic springs is tunable by adjusting the gap between the two magnet disks as shown in Fig. 1 where the stiffness (slope) depends on the setting of the gap between the two magnetic disks. In practice, we load a mass on a selected coil spring to make sure that the final loaded position reaches to the equilibrium, and then adjust the gaps of magnet springs. At the initial stage of the adjustment, we can firstly tune the gap just past the point of quasi-zero stiffness so that the instability of buckling in the QZS system is observed. Then we gradually release the gaps until the instability disappears and meanwhile the mass in oscillation initially can always rest on to the equilibrium position. Note that we can also gradually reduce the gaps just before the instability occurs. By so doing, we can achieve the best result of the QZS property in real experiments. The positive stiffness of coil spring depends on the size of loading mass, and the size of the permanent magnets depends on the stiffness of coil spring used because the ratio of the stiffness between the two types of springs must be remained the same once the geometric configuration is determined.

6. Conclusions

In this paper, we have carried out the theoretical and experimental investigation for a QZS vibration isolation system. Firstly a permanent magnet spring is introduced, and an approximate expression of repulsive force in the permanent magnet spring is proposed. This expression, although lacking causal relation, is perhaps accurate enough for most engineering applications, and makes the subsequent characteristic analysis easier with the simple and useful formulation.

Secondly, a novel prototype of a QZS vibration isolator with nonlinear magnetic springs is developed. The geometrical configuration for designing the unique feature of quasi-zero stiffness is described and the corresponding mathematical modeling is formulated. A series of static and dynamic characteristic analyses have been carried out which can be used for the future development of quasi-zero stiffness systems. This prototype provides a new method for the design of a low frequency vibration isolator. It is shown that there is a unique relationship between the stiffness of the vertical spring and distance between magnets that yields a QZS system. When the parameter configuration of QZS system is kept the same, changing the pre-stressed length δ can increase the loading capacity of the isolation mass. Moreover, in practical cases the approximate stiffness of QZS system can be used instead of the analytical stiffness in subsequent dynamic analysis. The relationship between the supported mass and the vertical spring is also discussed.

Thirdly, a numerical simulation to compare the QZS system and the linear system has been investigated. The characteristics of the system including the jumps in frequencies, transmissibility, attenuation limit for excitation force and the damping effect have all been discussed. Two approaches of the tuning procedure for adapting to the change of loading mass and quasi-zero stiffness are addressed, which are practically important to experimental investigations.

Finally, the experimental investigation carried out verifies the isolation performance of the QZS system. Experimental results show that the QZS system does not involve resonance phenomena as compared to the linear system. The excellent performance for attenuating the vibration of the proposed system can be largely extended to a lower frequency domain in comparison with the corresponding linear system.

Acknowledgment

The authors would like to appreciate Professor Shijian Zhu for his sincere help and support. This research work was supported by National Natural Science Foundation of China (11072075 and 11102026), Specialized Research Fund for the Doctoral Program of Higher Education (20110161120040), and the research grant (71075004) from the State Key Lab of Advanced Design and Manufacturing for Vehicle Body.

References

[1] A. Carrella, M.J. Brennan, T.P. Waters, Static analysis of a passive vibration isolator with quasi-zero-stiffness characteristic, *Journal of Sound and Vibration* 301 (2007) 678–689.
[2] I. Kovacic, M.J. Brennan, T.P. Waters, A study of a nonlinear vibration isolator with a quasi-zero stiffness characteristic, *Journal of Sound and Vibration* 315 (2008) 700–711.
[3] C.M. Harris, A.G. Piersol, *Shock and Vibrations Handbook*, McGraw Hill, New York, 2002.
[4] E.I. Rivin, *Passive Vibration Isolation*, ASME Press, New York, 2001.

[5] A. Carrella, M.J. Brennan, I. Kovacicb, T.P. Waters, On the force transmissibility of a vibration isolator with quasi-zero-stiffness, *Journal of Sound and Vibration* 322 (2009) 707–717.
[6] R.A. Ibrahim, Recent advances in nonlinear passive vibration isolators, *Journal of Sound and Vibration* 314 (2008) 371–452.
[7] X. Peng, D. Li, S. Chen, Quasi-zero stiffness vibration isolators and design for their elastic characteristics, *Journal of Vibration, Measurement and Diagnosis* 17 (1997) 44–46. (in Chinese).
[8] J.Z. Zhang, S. Dong, D. Li, Study on new type vibration isolation system based on combined positive and negative stiffness, *Nanotechnology and Precision Engineering* 2 (2004) 314–318. (in Chinese).
[9] J.Z. Zhang, D. Li, S. Dong, M.J. Chen, Development of new typed nonlinear ultra-low frequency horizontal vibration isolation system, *Journal of Machine Design* 22 (2005) 19–21. (in Chinese).
[10] D.L. Platus, Negative-stiffness-mechanism vibration isolation systems, *Proceedings of SPIE* 3786 (1999) 98–105.
[11] S. Santillan, L.N. Virgin, R.H. Plaut, Equilibria and vibration of a heavy pinched loop, *Journal of Sound and Vibration* 288 (2005) 81–90.
[12] L.N. Virgin, S.T. Santillan, R.H. Plaut, Vibration isolation using extreme geometric nonlinearity, *Journal of Sound and Vibration* 315 (2008) 721–731.
[13] C.M. Lee, V.N. Goverdovskiy, A.I. Temnikov, Design of springs with "negative" stiffness to improve vehicle driver vibration isolation, *Journal of Sound and Vibration* 302 (2007) 865–874.
[14] A. Carrella, M.J. Brennan, T.P. Waters, K. Shin, On the design of a high-static-low-dynamic stiffness isolator using linear mechanical springs and magnets, *Journal of Sound and Vibration* 315 (2008) 712–720.
[15] W.S. Robertson, B.S. Cazzolato, A.C. Zander, Nonlinear control of a one axis magnetic spring, *Proceedings of the 14th International Congress on Sound and Vibration*, 2007.
[16] W.S. Robertson, M.R.F. Kidner, B.S. Cazzdato, A.C. Zander, Theoretical design parameters for a quasi-zero stiffness magnetic spring for vibration isolation, *Journal of Sound and Vibration* 326 (2009) 88–103.
[17] N. Zhou, K. Liu, A tunable high-static-low-dynamic stiffness vibration isolator, *Journal of Sound and Vibration* 329 (2010) 1254–1273.
[18] W.D. Zhong, *Ferromagnetic Studies*, Beijing Science Press, 1998 (in Chinese).
[19] E.P. Furlani, A formula for the levitation force between magnetic disks, *IEEE Transactions on Magnetics* 29 (1993) 4165–4169.
[20] D. Vokoun, M. Beleggiab, L. Heller, P. Šittnera, Magnetostatic interactions and forces between cylindrical permanent magnets, *Journal of Magnetism and Magnetic Materials* 321 (2009) 3758–3763.
[21] W. Robertson, B. Cazzolato, A. Zander, A simplified force equation for coaxial cylindrical magnets and thin coils, *IEEE Transactions on Magnetics* 47 (2011) 2045–2049.
[22] I. Yamakawa, S. Takeda, H. Kojima, Behavior of a new type dynamic vibration absorber consisting of three permanent magnets, *Bulletin of the JSME* 20 (1977) 947–954.
[23] E. Bonisoli, A. Vigliani, Identification techniques applied to a passive elasto-magnetic suspension, *Mechanical Systems and Signal Processing* 21 (2007) 1479–1488.
[24] A.H. Nayfeh, *Introduction to Perturbation Techniques*, Wiley, New York, 1993.
[25] M.N. Hamdan, T.D. Burton, On the steady-state response of non-linear oscillators using harmonic balance, *Journal of Sound and Vibration* 166 (1993) 255–266.
[26] D.W. Jordan, P. Smith, *Nonlinear Ordinary Differential Equations*, third ed. Oxford, New York, 1999.
[27] S.M. Savaresi, C. Spelta, Mixed sky-hook and ADD: approaching the filtering limits of a semi-active suspension, *Journal of Dynamic Systems, Measurement, and Control* 129 (2007) 382–392.